0888-8809/07/$15.00/0
Printed in U.S.A.

Molecular Endocrinology 21(6):1312–1323

doi: 10.1210/me.2007-0113

In Vivo Imaging of Farnesoid X Receptor Activity Reveals the Ileum as the Primary Bile Acid Signaling Tissue

Sander M. Houten,* David H. Volle,* Carolyn L. Cummins, David J. Mangelsdorf, and Johan Auwerx

Institut de Génétique et Biologie Moléculaire et Cellulaire (S.M.H., D.H.V., J.A.), Centre National de la Recherche Scientifique/Institut National de la Santé et de la Recherche Médicale/Université Louis Pasteur, and Institut Clinique de la Souris (J.A.), 67404 Illkirch, France; Howard Hughes Medical Institute and Department of Pharmacology (C.L.C., D.J.M.), University of Texas Southwestern Medical Center, Dallas, Texas 75390; and Hôpitaux Universitaires de Strasbourg, Laboratoire de Biochimie Générale et Spécialisée (J.A.), 67000 Strasbourg, France

We generated and characterized a firefly luciferase reporter mouse for the nuclear receptor farnesoid X receptor (FXR). This FXR reporter mouse has basal luciferase expression in the terminal ileum, an organ with well-characterized FXRα signaling. *In vivo* luciferase activity reflected the diurnal activity pattern of the mouse, and is regulated by both natural (bile acids, chenodeoxycholic acid) and synthetic (GW4064) FXRα ligands. Moreover, *in vivo* and *in vitro* analysis showed luciferase activity after GW4064 administration in the liver, kidney, and adrenal gland, indicating that FXRα signaling is functional in these tissues. Hepatic luciferase activity was robustly induced in cholestatic mice, showing that FXRα signaling pathways are activated in this disease. In conclusion, we have developed an FXR reporter mouse that is useful to monitor FXRα signaling *in vivo* in health and disease. The use of this animal could facilitate the development of new therapeutic compounds that target FXRα in a tissue-specific manner. (*Molecular Endocrinology* 21: 1312–1323, 2007)

THE *IN VIVO* study of signaling pathways frequently relies on the analysis of the expression of downstream genes and the proteins they encode. Expression analysis requires access to tissues, which often requires killing of the animal, increasing animal use, and posing ethical problems. Furthermore, the expression of a given RNA and protein is frequently the end result of compound and converging signaling pathways, making it difficult to dissect the relative contribution of different signaling pathways to gene/protein levels. Noninvasive, quantitative, *in vivo* whole-body imaging of reporter animals that have been engineered to detect the activity of a signaling pathway offers many advantages compared with RNA and protein analysis. The technical evolution of whole-body imaging was catalyzed by the developments in the design and generation of genetically modified reporter animals, most notably mice, coupled with the rapid progress in noninvasive imaging technologies. Reporter animals can now be designed so that only a single signaling event, *e.g.* the activation of one transcription factor or nuclear receptor, is scored in a highly sensitive manner through the monitoring of a suitable reporter gene. The activity of reporter genes in response to a selected substrate will make it visible to the detector, allowing the collection of quantitative data on the spatial and temporal activities of the signaling pathway (1–3). Very sensitive *in vivo* imaging techniques, most notably positron emission tomography (6), single photon emission computed tomography (7), magnetic resonance imaging (8), and bioluminescence imaging with cooled charge-coupled device cameras (9–13) were optimized for the detection of reporter gene expression in small laboratory animals. Such strategies permit multiple consecutive analysis of the activity of a signaling pathway in the same animal that can therefore serve as its own control, reducing experimental variability and animal use.

A popular reporter gene for *in vitro* studies of gene expression is firefly (*Photinus pyralis*) luciferase. Over the past few years, luciferase has been used for imaging the *in vivo* activity of transcription factors, such as nuclear factor-κB (14–16) and hypoxia-inducible factor-1α (17), but also to score promoter activity (*e.g.* CYP3A4, heme oxygenase, inducible nitric oxide synthase, Vegfr2, and Hsp70) under different treatment conditions (18–22). In these studies, transgenic mice have been generated that carry the luciferase gene, placed under the control of a response element specific for the transcription factor of interest or a full-length promoter region of interest. After anesthesia,

First Published Online April 10, 2007

* S.M.H. and D.H.V. contributed equally to this work.

Abbreviations: CDCA, Chenodeoxycholic acid; CHX, cycloheximide; dLuc, destabilized luciferase; DMSO, dimethylsulfoxide; FXR, farnesoid X receptor; FXRE, FXR response element; IBABP, intestinal bile-acid binding protein; Luc, luciferase; NR, nuclear receptor; OST, organic solute transporter; SHP, short heterodimeric partner.

***Molecular Endocrinology* is published monthly by The Endocrine Society (http://www.endo-society.org), the foremost professional society serving the endocrine community.**

luciferase reporter mice are injected with the substrate of luciferase, luciferin. In the presence of luciferin, ATP, and molecular oxygen, luciferase emits photons with an average wavelength of 562 nm. These photons can penetrate tissues, allowing their external detection using a cooled charge-coupled device camera, although light from deeper tissues is more likely to be scattered and absorbed, making detection more difficult.

Luciferase imaging is well adapted for the functional characterization of nuclear receptors (NRs). Many NRs are ligand-gated transcription factors, which upon ligand binding, change conformation allowing the dissociation of corepressors and the recruitment of coactivators, resulting in the activation of transcription (23, 24). Knowledge of NR function is often based on the combination of information from pharmacological studies that involve administration of agonist or/and antagonist NR ligands to animals, and/or from the characterization of genetically engineered mouse models in which the expression of a NR is either induced via transgenesis or deleted via gene targeting strategies. Pharmacological and genetic approaches to characterize NR function fall short, however, in identifying those tissues in which NR signaling is active in the intact animal. Classically, such information was derived from the concurrence of the expression of a NR and of the presence of its cognate ligand in a given tissue. The fact that NR ligands are small lipophilic molecules, which are present in very low concentrations, make this approach challenging. More recently, noninvasive *in vivo* imaging has been successfully applied to monitor the activity of the estrogen (25, 26) and androgen receptor (27) *in vivo*. However, for most NRs, including the farnesoid X receptors (FXRα, NR1H4; FXRβ, NR1H5), this information is not available. FXRα is activated by conjugated and unconjugated bile acids (28–30), but also by androgen catabolites (31, 32). The main function of FXRα is to control genes involved in the enterohepatic recycling and detoxification of bile acids (33–35) as well as genes involved in metabolic homeostasis (23). This is in line with the reported expression pattern of FXRα in liver and intestine. Much less is known about FXRβ, for which functional orthologs have been identified in mouse, rat, dog, and rabbit, but not in humans and primates.

The aim of this study was to identify the tissues in which FXR signaling is active *in vivo*. To achieve this aim, we generated a transgenic FXR luciferase reporter mouse and characterized this mouse line *in vivo*. Our data establish that FXRα signaling is active beyond the entero-hepatic organs in kidney and adrenals. Furthermore, the FXR reporter mice illustrate that the ileum is the primary bile acid signaling tissue in the basal state, whereas FXRα signaling in the liver is only induced under pathological conditions, such as cholestasis. The FXR reporter mouse is a useful tool for the study of FXR biology and the characterization of new FXRα ligands.

RESULTS

Generation of a Destabilized Luciferase and a FXRα-Specific Reporter Plasmid

To accurately represent real-time imaging of gene expression, the reporter gene should ideally have a relatively short half-life. The reported half-life of firefly luciferase is 3 h in mammalian cells (36). In our hands, however, luciferase had an estimated half-life of 12 h. Such a stable Luciferase (Luc) protein will hamper the rapid detection of changes in gene expression. Therefore, we constructed a destabilized Luc (dLuc) by fusing the open reading frame of Luc to the rapid degradation domain of mouse ornithine decarboxylase (37). This region of the protein, which is rich in proline, glutamic acid, serine, and threonine, is called a PEST region (38). A similar strategy has been employed previously for destabilizing green fluorescent protein (39) and luciferase (40). Using Luc and dLuc, we created transgenic vectors with the following properties (Fig. 1A): 1) two chicken β-globin insulator sequences (41, 42) to prevent silencing of the transgene (43–45); 2) a minimal promoter derived from the Wnt-1 protooncogene promoter region harboring transcription initiation sites (46, 47); 3) an simian virus 40 late poly(A) signal that ensures polyadenylation of the (destabilized) luciferase mRNA; and 4) FXR and/or GAL4 response elements upstream of the Wnt-1 promoter to drive the expression of Luc or dLuc. The resulting transgenic vectors are named pdLucGAL4, pdLucFXR, pLucGAL4, and pLucFXR, and sequences have been deposited at GenBank (Fig. 1A).

We first characterized the stability of Luc and dLuc in transient transfections by using a synthetic transcription factor consisting of the GAL4 DNA-binding domain fused to the transactivation domain of the herpes simplex virus protein Vmw65 (GAL4-VP16). The resulting basal expression levels of dLuc were 7- and 9-fold lower in COS and HepG2 cells, respectively, indicating a 7- and 9-fold higher turnover of dLuc relative to Luc (Fig. 1B). To verify whether this reflected a difference in protein turnover, we treated transfected COS cells with cycloheximide (CHX) to inhibit protein synthesis, allowing the quantification of protein degradation. After CHX addition, dLuc activity decreased much faster than Luc activity (Fig. 1C). The decrease of dLuc followed first-order kinetics with a half-life of 1.7 h, whereas the estimated half-life of Luc was 12 h, perfectly reflecting the 7-fold difference in basal activity (Fig. 1B). In HepG2 cells, dLuc and Luc were more unstable with respective half-lives of 0.8 and 9.2 h (data not shown). Importantly, the difference in the stability of dLuc and Luc was only seen in living cells and not in cell lysates, as shown by a heat inactivation experiment (Fig. 1D). This proves that the difference in stability depends on living cells, and does not occur *in vitro* after the sample preparation. Immunoblot analysis of HepG2 cell lysates shows the difference in molecular weight of dLuc and Luc (64.7 *vs.* 60.4 kDa) (Fig. 1E).

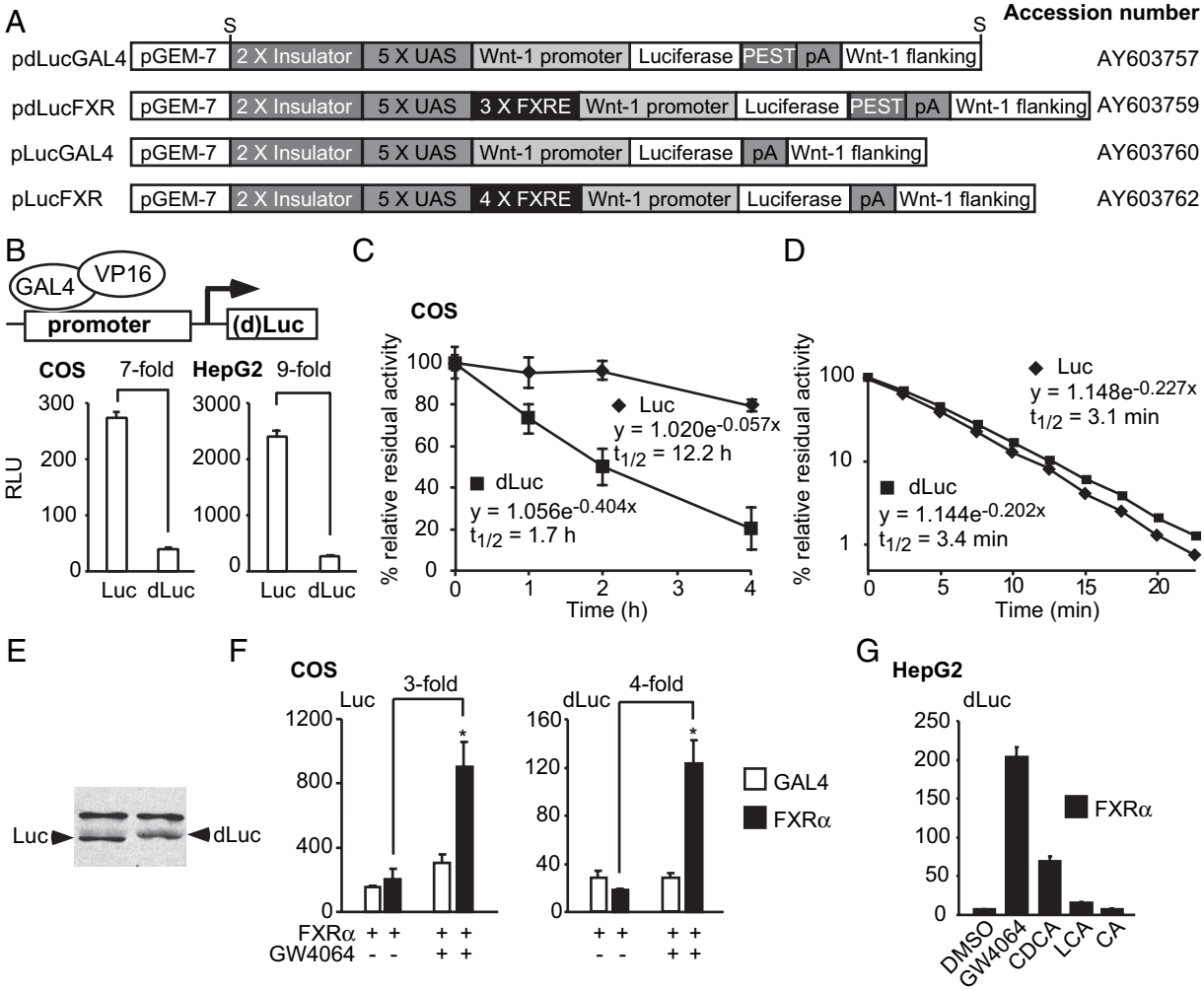

Fig. 1. Characterization of a Destabilized Luciferase and a FXRα-Specific Reporter Plasmid

A, Schematic representation of the constructs used for this study. S indicates the position of the *Sal*I site used for vector linearization. pA indicates the position of the polyadenylation site. UAS and FXRE denote the GAL4 and FXR response elements, respectively. B, Basal expression level of luciferase (Luc) and dLuc in COS and HepG2 cells. C, The stability of Luc and dLuc in COS cells after CHX addition. *Curves* were fitted to a first-order formula, and the half-life was calculated. D, Stability of Luc and dLuc during a heat inactivation experiment at 37 C. *Curves* were fitted to a first-order formula, and the half-life was calculated. E, Immunoblot analysis on lysates of HepG2 cells transfected with Luc or dLuc. The proteins migrated according to their calculated molecular weight: Luc, 60.6 kDa; dLuc, 64.7 kDa. F, Induction of (d)Luc activity in COS cells from the indicated reporter constructs after the addition of 1 μM synthetic FXRα agonist GW4064. G, Induction of dLuc activity in HepG2 cells from the FXRα reporter after the addition of natural [100 μM CDCA, lithocholic acid (LCA), and cholic acid (CA)] and synthetic FXRα ligands (1 μM GW4064).

To test the vectors as reporters for FXRα activity, we cotransfected COS cells with an FXRα expression vector and either pdLucGAL4, pdLucFXR, pLucGAL4, or pLucFXR, and subsequently treated cells with the FXRα-specific ligand GW4064. This yielded a 3- to 4-fold induction in pdLucFXR and pLucFXR and not in pdLucGAL4 and pLucGAL4 (Fig. 1F). As expected, the basal activity was higher in the Luc compared with the dLuc constructs (Fig. 1F). Finally, transfection of HepG2 cells with pdLucFXR and FXR yielded a 34-fold induction with GW4064, in addition to significant inductions by the natural FXRα agonist chenodeoxycholic acid (CDCA) and lithocholic acid (12- and 2-fold respectively) (Fig. 1G). Cholic acid, which is not a good *in vitro* ligand for FXRα, did not induce luciferase activity. These results prove that pdLucFXR and pLucFXR function as FXRα-specific reporters.

Generation of Transgenic FXR Reporter Animals

pdLucGAL4 and pdLucFXR were then used to generate transgenic mice. Five founders harboring the pdLucGAL4 transgene and six founders with the pdLucFXR transgene were selected for further characterization. The luciferase activity in the offspring of these founders was analyzed *in vivo* by imaging and *in vitro* by performing

luciferase assays in tissue extracts. The pdLucGAL4 transgenics showed almost no luciferase activity *in vivo*, except for the tail in some founders (data not shown). This was confirmed by the *in vitro* luciferase activity, which showed no detectable activity in tissues of founders 6, 17, and 30 and some activity in tissues of founder 21 and 27 (supplemental Table 1, published as supplemental data on The Endocrine Society's Journals Online web site at http://mend.endojournals.org). Two pdLucFXR transgenics showed *in vivo* luciferase activity in the abdomen, with founder 61 having more activity than founder 2 (data not shown). *In vitro* analysis of organs of pdLucFXR mice showed barely detectable luciferase activity in the four other founders, although stomach and tail in two founders had considerable activity (supplemental Table 2, published as supplemental data on The Endocrine Society's Journals Online web site at http://mend.endojournals.org). Founder 61 had activity in the entire gastrointestinal tract, with specific luciferase activity increasing from duodenum to colon (supplemental Table 2), confirming the abdominal localization of the *in vivo* luciferase activity. In addition, we found high luciferase activity in the keratinized part of the stomach, the testicle, and the tail (supplemental Table 2). High luciferase activity was also found in the keratinized part of the stomach, the testicle, and the tail of founder 2 (supplemental Table 2). Most interesting was the localization of the luciferase activity in the ileum (supplemental Table 2), a part of the intestine with an important role in bile acid physiology and active FXRα signaling. Therefore, we chose to characterize this founder in more detail.

Characterization of a Transgenic FXR Reporter

To verify whether our FXR reporter mouse responds to a natural FXRα agonist, we analyzed these mice on a normal chow diet. *In vivo* imaging during the light phase revealed low luciferase activity in the abdomen in the region corresponding to the ileum (Fig. 2, A and B, and supplemental Table 2). Upon switching these mice to a similar diet containing 0.5% CDCA, two of the three mice showed an increase of the luminescence in the abdomen in the region corresponding

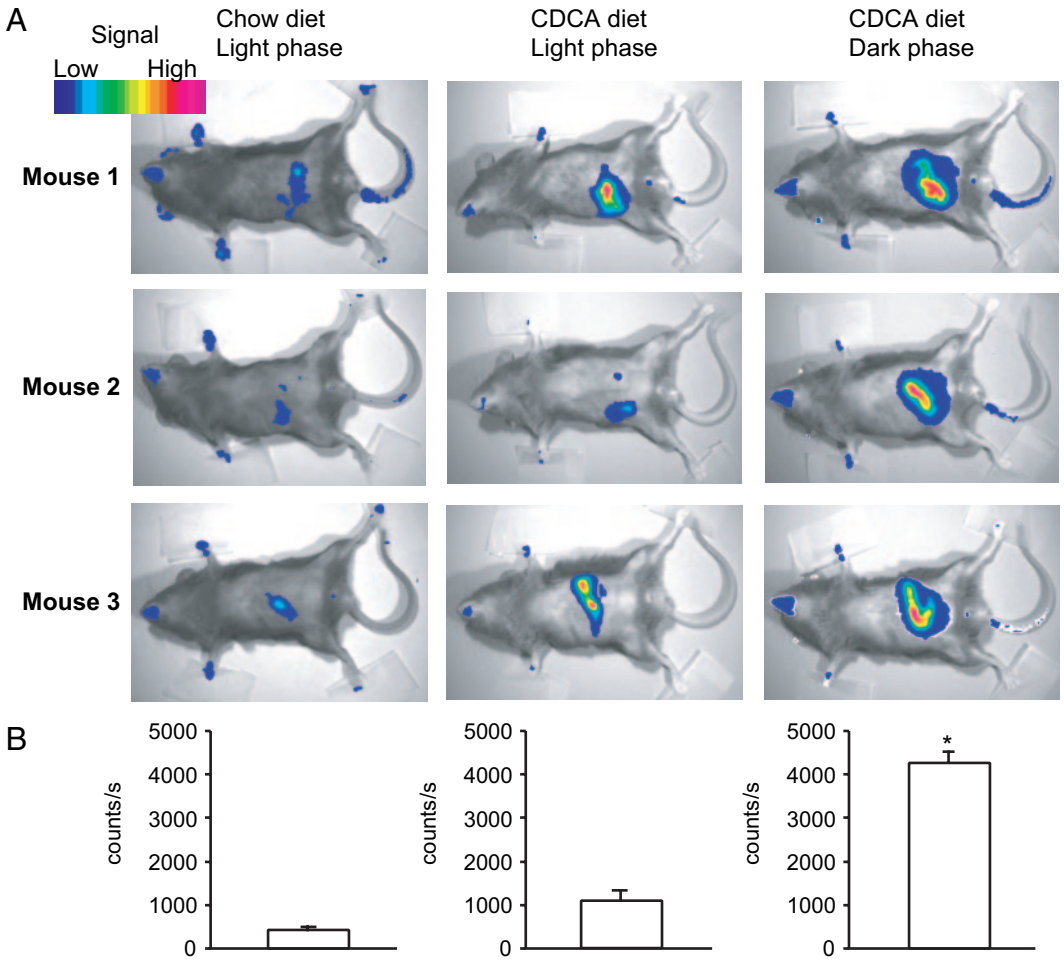

Fig. 2. *In Vivo* Imaging of FXR Activity in Mice on a CDCA-Containing Diet

A, *In vivo* images of luciferase activity in male FXR reporter mice under the conditions displayed in the figure. B, Histogram of the quantification of the signal.

most likely to the ileum (Fig. 2, A and B). Because mice usually do not forage during their inactive period, we also imaged the mice on the CDCA diet during the dark phase. This showed a significant increase in the luciferase activity in the abdominal region (Fig. 2, A and B). No activity was detected in the region of the liver. This result shows that the luciferase activity in the FXR reporter mice is regulated by natural ligands. Moreover, it suggests that FXR activity reflects diurnal activity pattern. In an independent experiment, we investigated the diurnal variation in luciferase activity on a normal chow diet. During the active dark period, luciferase activity in the abdominal region was 1.8-fold higher than during the light period ($P = 0.003$) (Fig. 3, A and B). This shows that the FXR activity follows the activity pattern of the mouse. During the dark period on chow, luciferase activity remained lower than on the CDCA diet, showing that this bile acid potently induced FXR activity in the abdomen.

We treated the FXR reporter animals with the synthetic FXRα-specific ligand GW4064. Due to the suboptimal pharmacokinetic properties of this drug, it is difficult to obtain high plasma levels. Indeed, ip injection of a GW4064 emulsion in peanut oil only modestly increased the signal in the abdominal region after 4–8 h. No increase in the region of the liver was observed (data not shown). GW4064 is very soluble in dimethylsulfoxide (DMSO); therefore, we injected FXRα reporter mice with a GW4064 solution in DMSO or DMSO only. Four hours after injection, the animals were imaged followed by dissection for *in vitro* analyses of luciferase activity in selected organs. In the vehicle-treated mice, low luciferase activity was visible in the abdomen in the region corresponding to the ileum (Fig. 4A and supplemental Table 2). After injection with GW4064, luciferase activity was dramatically increased in the abdomen in regions not only corresponding to the ileum but also to the liver (Fig. 4A). Indeed, *in vitro* analysis of selected potential FXRα target tissues revealed significant induction of luciferase activity by GW4064 in the distal part of the ileum, the kidneys, the adrenals, and the liver (Fig. 4B). All four organs express high levels of FXRα (48). Proximal parts of the small intestine also showed detectable luciferase activity after GW4064 administration. This experiment validates our model as an FXR reporter in the enterohepatic tissues. It also suggests that FXRα can be func-

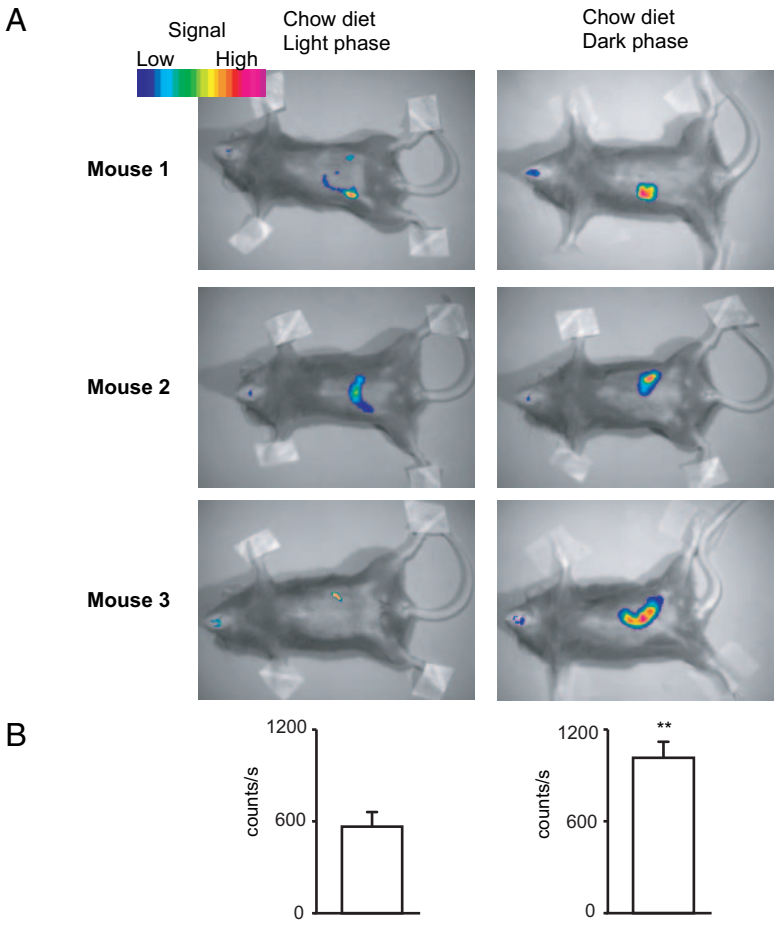

Fig. 3. *In Vivo* Imaging of Diurnal Variation in FXR Activity

A, *In vivo* images of luciferase activity in female FXR reporter mice (n = 9) under the conditions displayed in the figure. Representative images are shown. B, Histogram of the quantification of the signal in 9 mice.

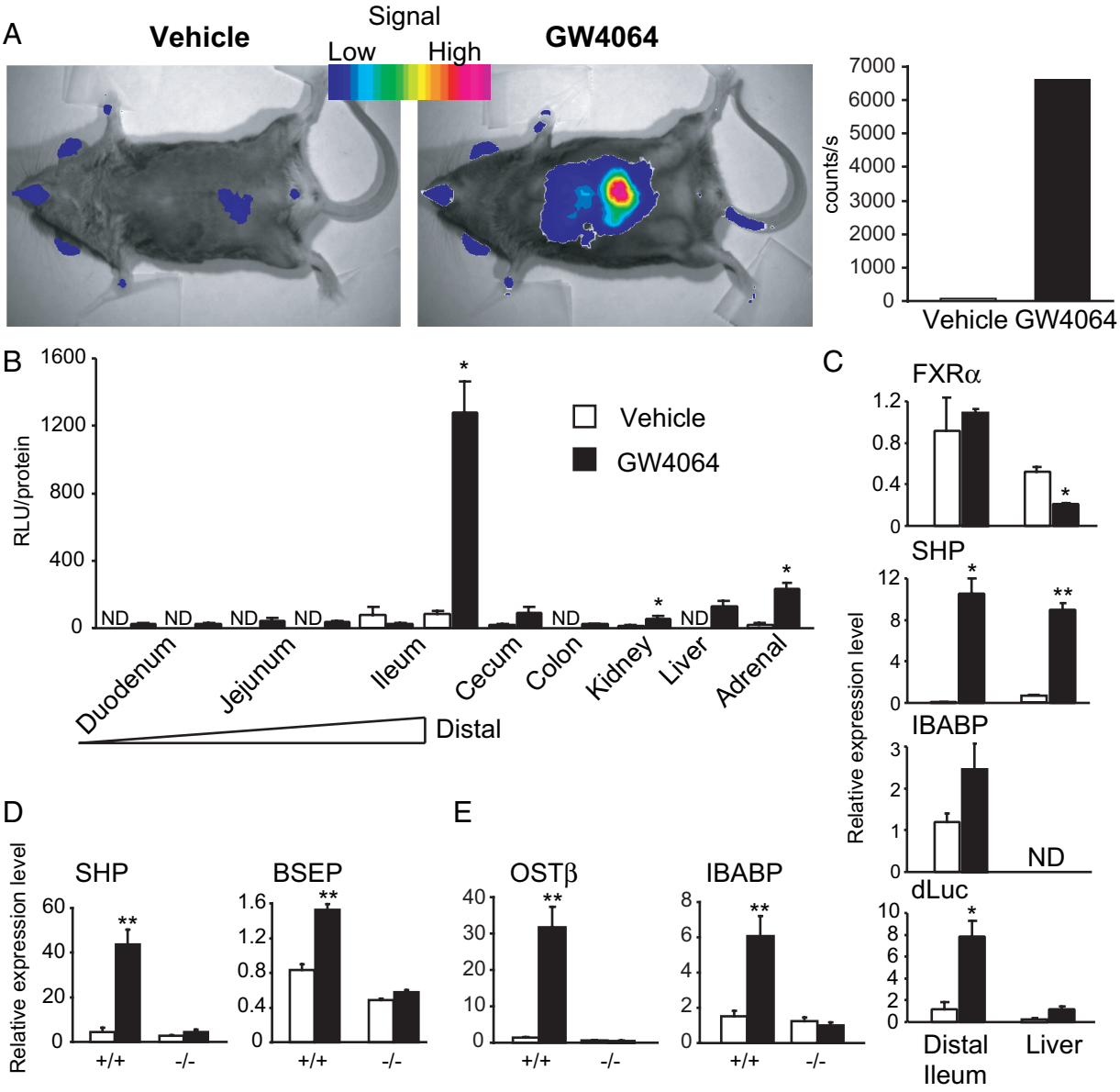

Fig. 4. *In Vivo* and *in Vitro* FXR Activity after Activation with a Synthetic Ligand

A, *In vivo* images of luciferase activity in male FXR reporter mice after injection of the synthetic FXRα-specific ligand GW4064 or vehicle. The histogram is the quantification of the signal. B, *In vitro* luciferase activity in selected organs of female FXR reporter mice after injection with the synthetic FXRα-specific ligand GW4064 or vehicle. C, Expression levels of selected FXRα target genes and dLuc in the distal ileum and liver of FXR reporter mice after injection with the synthetic FXRα-specific ligand GW4064 or vehicle. D, Expression levels of selected FXRα target genes in liver of FXRα knockout mice and wild-type littermates after injection with the synthetic FXRα-specific ligand GW4064 or the vehicle DMSO. E, Expression levels of OSTβ and IBABP in adrenal of FXRα knockout mice and wild-type littermates after injection with the synthetic FXRα-specific ligand GW4064 or the vehicle DMSO.

tional in tissues that are not directly involved in bile acid metabolism, such as the adrenal gland, which expresses FXRα in the adrenal cortex (48, 49).

We also validated our model at the transcriptional level. As reported before, FXRα is expressed at high levels in the distal ileum and the liver (48, 49). GW4064 treatment significantly decreased FXRα expression in the liver (Fig. 4C). FXRα target genes such as intestinal bile-acid binding protein (IBABP) and short heterodimeric partner (SHP; NR0B2) were induced by GW4064 treatment (Fig. 4C). Because IBABP is specific to the distal ileum, its expression was not detected in the liver (Fig. 4C). Hepatic CYP7A1 was down-regulated by GW4064 treatment (data not shown). Luciferase mRNA was induced in liver and distal ileum by GW4064 treatment. The induction of luciferase in the terminal ileum was higher than the induction of IBABP expression (Fig. 4C). A likely ex-

planation for this is the presence of three FXR response elements (FXREs) in the dLuc gene promoter. The induction of dLuc in liver is 3-fold but was not statistically significant due to the almost undetectable mRNA levels in the untreated group (Fig. 4C).

To confirm whether administration of GW4064 dissolved in DMSO gives specific FXRα activation, we used FXR$\alpha^{-/-}$ mice. FXR$\alpha^{-/-}$ and wild-type littermates were injected with GW4064 or DMSO alone and killed 4 h later. Treatment with GW4064 induced SHP and bile salt export pump (BSEP) expression in the liver of wild-type mice as observed in the FXRα reporter animals, but this induction was absent in FXR$\alpha^{-/-}$ mice (Fig. 4D). FXRα activation also down-regulated CYP7A1 (data not shown). This shows that ip administration of GW4064 in DMSO results in the specific activation of FXRα in the liver. We also verified whether GW4064 could give specific FXRα activation in the adrenal gland responsible for the increased luciferase activity in the FXR reporter mouse (Fig. 4B). Treatment with GW4064 specifically induced organic solute transporter β (OSTβ) in wild-type animals, but not in FXR$\alpha^{-/-}$ mice. In addition, expression of IBABP, which is expressed at very low levels in the adrenal, was induced in an FXRα-dependent manner (Fig. 4E). Combined, these results indicate that FXRα can be functional in the adrenal.

Imaging of Hepatic FXR Activity after Bile Duct Ligation

We used the FXR reporter mouse to monitor hepatic FXRα activation after cholestasis. To induce cholestasis, the cystic and common bile ducts were ligated, and the mice were imaged 6 and 24 h after this operation. Six hours after bile duct ligation, luciferase activity *in vivo* and *in vitro* was only minimally increased (data not shown). After 24 h, luminescence in the hepatic region was increased in bile duct-ligated mice, whereas no *in vivo* luciferase activity was detected in the hepatic region of sham-operated mice. These observations were confirmed by *in vitro* luciferase measurements (Fig. 5). Cholestasis in bile duct ligated mice was evidenced by increased plasma liver enzymes and bile acid levels (Fig. 5). These data show that, in contrast to the situation in the ileum, hepatic

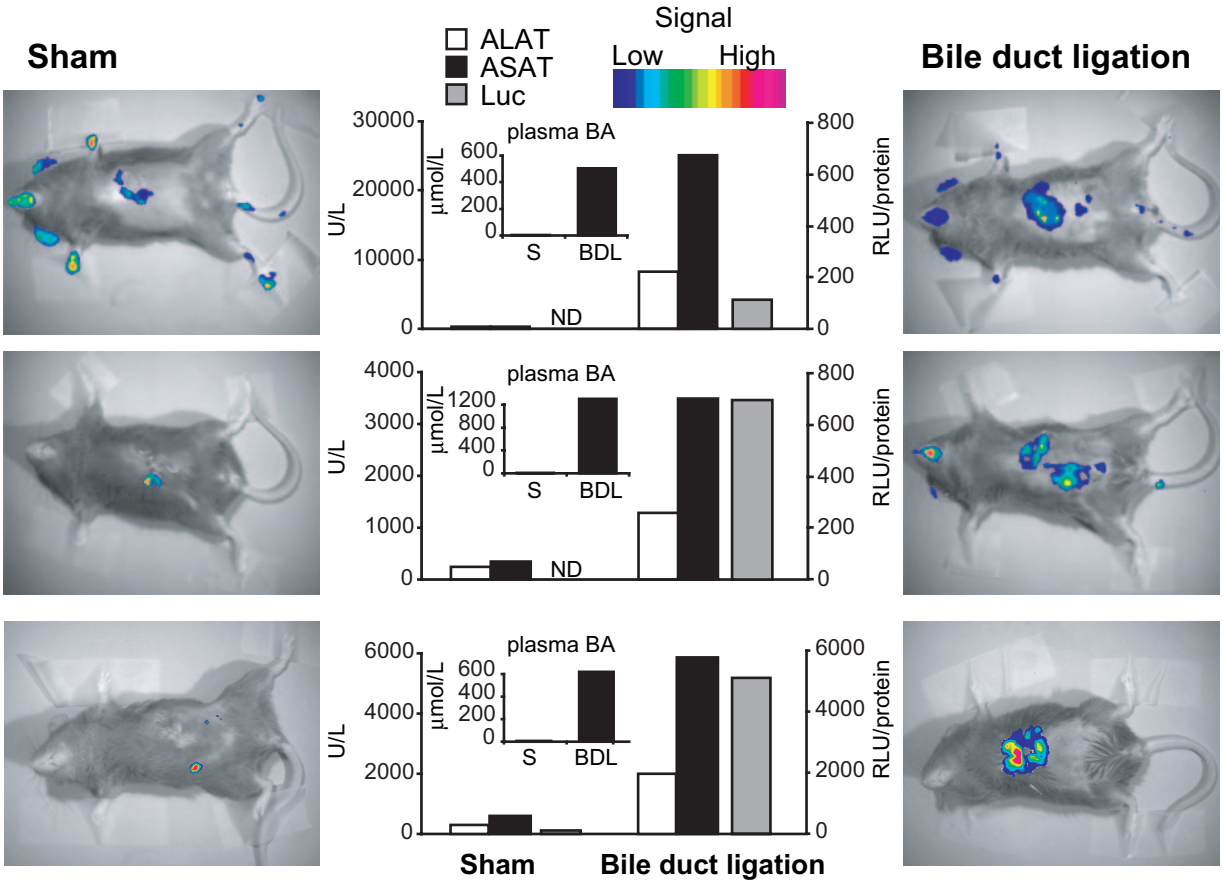

Fig. 5. *In Vivo* Imaging of FXR Activity in Mice after Bile Duct Ligation

In vivo images of luciferase activity in male and female FXR reporter mice after sham operation or bile duct ligation. Three independent experiments were performed. Each couple of mice is a representative for each of these experiments. The histogram displays the plasma liver enzymes in units per liter (U/L) and the *in vitro* hepatic luciferase activity in relative light units (RLU) per 50 μg protein. Plasma bile acids are in the *inset*. BA, Bile acid; BDL, bile duct ligation.

FXRα is silent under basal conditions, but is robustly activated during cholestasis.

DISCUSSION

Here, we report the generation and characterization of a firefly luciferase reporter mouse for the nuclear receptor FXR. This is the first reporter mouse employing a dLuc to study nuclear receptor signaling allowing the detection of changes more rapidly than with the classical luciferase. Of six pdLucFXR transgenic founders tested, only one was suitable for the reporter studies. A possible explanation for this relatively low success rate could be the random insertion of our transgene in the genome and insufficient protection from the β-globin insulator against position effects. Another potential problem could be low luciferase protein levels due to the use of the dLuc. pdLucGAL4 and pdLucFXR transgenics have background expression of dLuc in several different tissues depending on the founder studied. Background expression in the tail was consistent in several founders and can potentially be explained by the choice for the first 927 bp derived from the Wnt-1 protooncogene promoter region as a minimal promoter.

In theory, the luciferase activity in our FXR reporter mouse could also be induced by FXRβ, because both receptors bind to IR1 response elements in the promoter of their target genes. FXRβ is a nuclear receptor that has a relatively high degree of homology with FXRα (50). FXRβ functional orthologs have been identified in mouse, rat, dog, and rabbit, but only pseudogenes have been found in humans and primates. Although lanosterol has been identified as a ligand for FXRβ, nothing is known about the physiological function of this nuclear receptor (50). Murine FXRβ has recently been shown to be expressed at low levels in liver and testis (49). Based on the current literature, we cannot formally exclude a role for FXRβ in the activation of luciferase in our *in vivo* model.

The specificity of our reporter system has been demonstrated using both natural (CDCA) and synthetic (GW4064) FXRα agonists. After CDCA administration, luciferase was specifically induced in the intestine. In response to GW4064, we observed luciferase induction in the terminal ileum and liver by *in vivo* imaging, making our model an attractive tool for the development of new (synthetic) FXRα ligands or modulators. Moreover, *in vitro* analysis after GW4064 administration showed induction of luciferase activity in kidney and adrenal, both organs that express FXRα, indicating that FXRα can be functional in these tissues and that it can drive the expression of target genes.

Our FXR reporter mouse is also useful to study the function of FXR under physiological and pathological conditions. We have shown low basal luciferase expression and activity in the terminal ileum, an organ that encounters high levels of bile acids and has well-characterized FXRα signaling. After CDCA administration, the luciferase activity in the ileum is induced and followed the diurnal activity pattern of the mouse. On a chow diet, luciferase activity also followed the diurnal activity pattern, most probably reflecting foraging during the active dark period. Our FXR reporter model has no detectable basal luciferase activity in the liver, even after feeding a diet containing CDCA (Fig. 2). This is surprising because the liver plays an important role in bile acid homeostasis, and CDCA administration is known to activate FXRα target genes in the liver. There are multiple possible explanations for this. First, dLuc protein in the liver could be more unstable when compared with intestine, because the stability of dLuc in HepG2 cells was slightly lower than in COS cells. In addition, our transgene could be located in a genomic locus that is relatively inactive in the liver. Alternatively, it could indicate that hepatic FXRα is only activated when bile acid levels are pathologically elevated. Consistent with this latter hypothesis, we show that, after bile duct ligation, which results in the hepatic accumulation of supraphysiological levels of bile acids, luciferase activity in the liver is induced in the FXR reporter mouse. The absence or the weak intensity of the luciferase signal in the liver of the FXR reporter mice under basal conditions, is in sharp contrast to the basal luciferase activity detected in the ileum. In the liver, bile acid-mediated activation of FXRα induces the expression of the atypical NR, SHP, which acts as a NR corepressor. SHP potently inhibits of the activity of the liver receptor homolog 1 (LRH-1; NR5A2) and the liver X receptors (LXRs; NR1H2/3) to induce the expression of CYP7A1, the rate-limiting enzyme in bile acid synthesis. Induction of SHP expression, subsequent to the exogeneous administration of bile acids, was hence proposed to be responsible for the feedback inhibition of bile acid production (51, 52). Under basal conditions (without added bile acids), the levels of bile acids in the liver seem unable to activate FXRα signaling, calling into question the proposed role of hepatic FXRα in the feedback inhibition of bile acid signaling under basal homeostatic conditions. The terminal ileum, the tissue with the highest level of FXRα signaling under physiological conditions, may be more important in mediating the feedback inhibition of bile acid synthesis. This would support the recent finding that FGF-15-mediated down-regulation of CYP7A1 expression is the primary pathway for inhibition of bile acid biosynthesis (53).

Although the function of FXRα in the adrenal gland remains unknown, luciferase activity increased in this organ after GW4064 administration. An FXRα-dependent response to GW4064 in this organ was only observed for OSTβ and IBABP and not for the classic FXRα target SHP (data not shown). IBABP is an intestinal gene and is only expressed at very low levels in the adrenal, whereas OSTs have previously been shown to be induced by GW4064 in an adrenal organ culture model (54). This proves that using pharmacological activation, FXRα in the adrenal can be activated. It is interesting that, in addition to bile acids, androgen catabolites like dehydroepiandrosterone,

androstenedione, dihydrotestosterone, androsterone, and etiocholanolone were reported to activate FXRα (31, 32), although at nonphysiological concentrations. It would be interesting to test the effect of these androgen catabolites in the FXRα knockout and the FXR reporter mouse to validate them as *bona fide* FXR ligands.

In conclusion, we have developed a FXR luciferase reporter mouse that is useful to monitor *in vivo* physiological and pathological FXRα signaling and to develop new FXRα agonist or modulators.

MATERIALS AND METHODS

Materials

D-Luciferin was obtained from Euromedex (Mundolsheim, France). Rabbit antiluciferase and CDCA were obtained from Sigma. GW4064 was a kind gift from Margrit Schwarz (Hoffmann-La Roche, Basel, Switzerland).

Cloning Procedures

dLuc was obtained by modifying the luciferase gene in the pGL3 basic vector (Promega, Madison, WI). The mouse ornithine decarboxylase rapid degradation domain was amplified from pd2EGFP-1 (Clontech, Mountain View, CA) with primers 5′-g AgC CAT ggC TTC CCg CCg g-3′ and 5′-ATg ATC TAg AgT CgC ggC Cg-3′. This fragment was incubated with Mung Bean Nuclease and digested with *Xba*I. The Ochre stop codon of luciferase was mutated into a serine using primers 5′-CgA CgA TgA CgC Cgg TgA AC-3′ and 5′-CgA CTC TAg AAT gAC ACg gCg ATC TTT CCg-3′. This fragment was incubated with Mung Bean Nuclease and digested with *Xba*I and *Sgr*AI. The resulting fragments were ligated into the *Sgr*AI and *Xba*I sites of pGL3 basic. As a result, we obtained one in-frame fusion protein that was missing three nucleotides encoding a leucine (TTg) at the transition between the open reading frames. This is probably due to aspecific nuclease activity of the Mung Bean Nuclease. By mutating E558, E560, and E561 to alanines using primer 5′-gC CAT ggC TTC CCg CCg gCg gTg gCg gCg CAg gAT gAT ggC ACg CTg C-3′, we obtained the dLuc used for this study.

The transgenic vectors were obtained by modifying a vector named Bigenic UAS-Wnt-1 (a gift from Dr. T. Perlmann, Ludwig Institute for Cancer Research, Stockholm, Sweden). The dLuc or Luc open reading frame including the simian virus 40 late poly(A) signal was released from pGL3 using *Hin*dIII and *Acc*I. The *Hin*dIII was blunted, and the resulting fragment was ligated in the *Eco*RV and *Cla*I sites of the Bigenic UAS-Wnt-1 vector. The resulting vector contains two *Not*I sites. The *Not*I site derived from the mouse ornithine decarboxylase rapid degradation domain was destroyed by ligation of a small double-stranded oligo in this site. The other *Not*I, positioned just beside five GAL4 upstream activating sequences, was used to ligate a double-stranded oligo with an FXRE (5′-ggC CgC Tgg ggC Ag**A ggT CA**g **TgA CCT** CTC Tgg gCC CAT gCC A**Ag gTC A**g**T gAC CT**C TCT-3′ and 5′-g gCC AgA g**Ag gTC A**C**T gAC CT**T ggC ATg ggC CCA gAg **Agg TCA** C**Tg ACC T**CT gCC CCA gC-3′). The inverted repeat spaced by 1 nucleotide (IR1) sequence is shown in bold. The oligo leaves the *Not*I site intact and was ligated in the vector two times. The resulting transgenic vectors are named pdLucGAL4 (GenBank accession no. AY603757), pdLucFXR (AY603759), pLucGAL4 (AY603760), and pLucFXR (AY603762).

pSG5-mFXRα4 was obtained by PCR amplification of mouse FXRα4 from liver cDNA using the primers 5′-A CgC ggA TCC Agg ATg gTg ATg CAg TTT CAg gg-3′ and 5′-CgC gCT AgC CCA CTg gTg TCC ATC ACT gC-3′. The primers introduce a *Bam*HI site (underlined). The PCR product was cloned into pSG5 (Stratagene, La Jolla, CA) using the *Bam*HI site and a blunted *Bgl*II site.

Transient Transfection and Luciferase Assays

HepG2 (ECACC) and COS-1 cells were transfected in 48-well plates using lipofectamine (Invitrogen, Cergy Pontoise, France) or TransFast (Promega). Each well contained 100 ng luciferase reporter and 50 ng β-galactosidase expression plasmid. When indicated, we transfected 20 ng GAL4-VP16 or 20 ng FXRα4 and 2 ng RXRα expression plasmid. Ligands for FXRα were dissolved in DMSO and added to the cells. CHX was dissolved in ethanol and used at a concentration of 100 μg/ml. Luciferase measurements were normalized to β-galactosidase activity. Cells were maintained at 37 C in a humidified atmosphere of 5% CO_2.

Western Blot Analysis

Protein extracts were subjected to SDS-PAGE and transferred onto a nitrocellulose membrane (Amersham Biosciences, Piscataway, NJ). Membranes were incubated overnight at 4 C with primary polyclonal antibodies raised against luciferase followed by a 1-h incubation with a peroxidase-conjugated antirabbit or antimouse IgG (Roche Diagnostics, Meylan, France). Peroxidase activity was detected using the Western Light System (PerkinElmer Life Sciences, Courtaboeuf, France).

Biochemical Analysis

Alanine amino transferase and aspartate amino transferase were measured using specific assays (Boehringer-Mannheim, Mannheim, Germany) on an Olympus automated analyzer. Plasma bile acids were measured using an enzymatic assay from Randox (Crumlin, UK).

Transgenic Mice

All animal experiments were approved by institutional committees. To remove the pGEM-7 backbone of the transgenic vectors, the plasmids were linearized using *Sal*I and purified after gel electrophoresis. Transgenic mouse lines were obtained after pronuclear DNA injection according to established procedures (55). Screening for founders and routine genotyping was performed by PCR on genomic DNA isolated from the tail using primers 5′-taa gag gcc tat aag agg cgg-3′ and 5′-tgg cgt ctt cca tgg tgg ct-3′. In mice carrying the transgene, this PCR yields a 269-bp product. The transgene was kept in a hemizygous state by crossing founders and their offspring with C57BL/6J mice. For the characterization of founders, mice were treated for 4 h with GW4064. For this, GW4064 was dissolved in DMSO and 100 μl was injected ip at a dose of 30 mg/kg. For feeding of CDCA, normal chow was mixed with 0.5% CDCA. Before switching from chow to CDCA-containing diet, the animals were fasted overnight to prevent taste aversion. Images in light phase were made 24 h after refeeding. Image in dark phase were made 84 h after refeeding. To verify CDCA intake, food intake and body weight were measured daily. For analysis of luciferase activity during the diurnal activity pattern, mice ($n = 9$) were imaged at 1400 and 0200 h, which is at the middle of their light and dark phase, respectively. After the imaging, the mice were allowed to recover from anesthesia for at least 10 d before the next round of imaging.

FXR$\alpha^{-/-}$ Mice

The FXR$\alpha^{-/-}$ mice (4) were bred on a pure 129 background by backcrossing 10 generations to 129/SvEv mice. The wild types were generated from heterozygote crosses after the 10th backcross. All animals were male and between 4 and 5.5 months of age.

Bile Duct Ligation

Mice were anesthetized using 7.5 mg/kg Rompun and 50 mg/kg ketamine ip, and the abdomen was shaved. Liver was pulled out a small abdominal incision followed by a ligation of the cystic and the common duct using sutures. The abdominal incisions were closed in two layers. Sham-operated mice underwent exactly the same procedure with the exception of the closing of the ligation.

In Vitro Luciferase Assay

Selected tissues were homogenized in lysis buffer [25 mM Tris·Cl (pH 7.8), 2 mM EDTA, 1 mM dithiothreitol, 10% glycerol, 1% Triton X-100 supplemented with the protease inhibitors phenylmethylsulfonylfluoride, antipain, chymostatin, pepstatin, aprotinin, and leupeptin] using an Ultra-Turrax (Janke & Kunkel, Staufen, Germany). Homogenates were centrifuged for 5 min at 11,000 $\times$ *g*. The protein concentration in the supernatant was determined by the Bradford (Bio-Rad, Hercules, CA) assay. All tissues were diluted to 2 mg/ml protein in lysis buffer. Luciferase was assayed using 25 μl tissue lysate and 50 μl assay buffer [20 mM Tris·Cl (pH 7.8), 1.1 mM $MgCl_2$, 2.7 mM $MgSO_4$, 0.1 mM EDTA, 33.3 mM dithiothreitol, 530 μM ATP, 400 μM luciferin, and 210 μM coenzyme A] on a Berthold Technologies (Bad Wildbad, Germany) MicroLumat LB 96 P luminometer. The bile duct ligation samples were measured on a BertholdTech CENTRO XS3 LB 960, which is more sensitive. The relative light units emitted over a 9-sec period were integrated. Transfected cells were lysed in lysis buffer and analyzed in a similar way.

Imaging

In vivo visualization of luciferase expression was performed with a −70 C Peltier cooled charged-coupled device camera (NightOWL LB 981; Berthold Technologies). Images were acquired and processed using the WinLight32 software (Berthold Technologies). Just before imaging, mice were anesthetized using 15 mg/kg Rompun and 99 mg/kg ketamine, ip; the abdomen was shaved; and 60 μl of D-luciferin (Euromedex, Mundolsheim, France) in water was injected at a dose of 120 mg/kg. Directly after the luciferin injection, the mice were placed under the camera and a sequence of two images (exposure, 5 min) was taken. Background was corrected, and the second image was used for quantitative analysis.

Expression Level Analysis

Total RNA from liver and ileum was extracted from frozen tissue samples using RNA-solv reagent (Omega Biotek, Doraville, GA). cDNA synthesis and real-time PCR measurement were done as described before (5). For the experiment using FXR$\alpha^{-/-}$ mice, expression analysis was performed as described in Ref. 49. The sequences of the primer sets used are available at the following URL: http://www.igbmc.u-strasbg.fr/recherche/DepGPSN/Eq_JAuwe/Publi/Paper.html.

Statistical Analysis

Values were reported as mean ± SE. Statistical differences were determined by a Student's *t* test. Statistical significance is displayed as follows: *, $P < 0.05$; or **, $P < 0.01$.

Acknowledgments

We thank Maria Cristina Antal and Andrée Krust for discussions and technical assistance, Margrit Schwarz for the supply of GW4064, Thomas Perlmann for the bigenic UAS-Wnt-1 Vector, and Erwan Garo for help with the bile duct ligation.

Received February 28, 2007. Accepted April 4, 2007.

Address all correspondence and requests for reprints to: Johan Auwerx, Institut de Génétique et Biologie Moléculaire et Cellulaire, 1 Rue Laurent Fries, Parc d'Innovation, 67404 Illkirch, France. E-mail: auwerx@igbmc.u-strasbg.fr.

This work was supported by fellowships of the European Molecular Biology Organization (EMBO) and the Fondation Recherche Médicale (FRM) (to S.M.H.). D.J.M. is an Investigator and C.L.C. is an Associate of the Howard Hughes Medical Institute (HHMI). Work in the laboratory of J.A. was supported by grants from Agence Nationale de la Recherche, Centre National de la Recherche Scientifique, Institut National de la Santé et de la Recherche Médicale, Université Louis Pasteur, Hôpital Universitaire de Strasbourg, National Institutes of Health (NIH), EMBO, FRM, and the European Union (QLRT-2001-00930 and LSHM-CT-2004-512013), and in the laboratory of D.J.M. by grants from HHMI, the Robert A. Welch Foundation, and NIH (U19-DK62434).

Disclosure statement: The authors have nothing to disclose.

REFERENCES

1. Gross S, Piwnica-Worms D 2005 Spying on cancer: molecular imaging in vivo with genetically encoded reporters. Cancer Cell 7:5–15
2. Massoud TF, Gambhir SS 2003 Molecular imaging in living subjects: seeing fundamental biological processes in a new light. Genes Dev 17:545–580
3. Weissleder R 2002 Scaling down imaging: molecular mapping of cancer in mice. Nat Rev Cancer 2:11–18
4. Sinal CJ, Tohkin M, Miyata M, Ward JM, Lambert G, Gonzalez FJ 2000 Targeted disruption of the nuclear receptor FXR/BAR impairs bile acid and lipid homeostasis. Cell 102:731–744
5. Watanabe M, Houten SM, Wang L, Moschetta A, Mangelsdorf DJ, Heyman RA, Moore DD, Auwerx J 2004 Bile acids lower triglyceride levels via a pathway involving FXR, SHP, and SREBP-1c. J Clin Invest 113: 1408–1418
6. Phelps ME 2000 Inaugural article: positron emission tomography provides molecular imaging of biological processes. Proc Natl Acad Sci USA 97:9226–9233
7. Gambhir SS, Herschman HR, Cherry SR, Barrio JR, Satyamurthy N, Toyokuni T, Phelps ME, Larson SM, Balatoni J, Finn R, Sadelain M, Tjuvajev J, Blasberg R 2000 Imaging transgene expression with radionuclide imaging technologies. Neoplasia 2:118–138
8. Genove G, Demarco U, Xu H, Goins WF, Ahrens ET 2005 A new transgene reporter for in vivo magnetic resonance imaging. Nat Med 11:450–454

9. Contag CH, Spilman SD, Contag PR, Oshiro M, Eames B, Dennery P, Stevenson DK, Benaron DA 1997 Visualizing gene expression in living mammals using a bioluminescent reporter. Photochem Photobiol 66:523–531
10. Contag PR, Olomu IN, Stevenson DK, Contag CH 1998 Bioluminescent indicators in living mammals. Nat Med 4:245–247
11. Honigman A, Zeira E, Ohana P, Abramovitz R, Tavor E, Bar I, Zilberman Y, Rabinovsky R, Gazit D, Joseph A, Panet A, Shai E, Palmon A, Laster M, Galun E 2001 Imaging transgene expression in live animals. Mol Ther 4:239–249
12. Wu JC, Sundaresan G, Iyer M, Gambhir SS 2001 Noninvasive optical imaging of firefly luciferase reporter gene expression in skeletal muscles of living mice. Mol Ther 4:297–306
13. Bhaumik S, Gambhir SS 2002 Optical imaging of *Renilla* luciferase reporter gene expression in living mice. Proc Natl Acad Sci USA 99:377–382
14. Carlsen H, Moskaug JO, Fromm SH, Blomhoff R 2002 In vivo imaging of NF-κB activity. J Immunol 168: 1441–1446
15. Sadikot RT, Wudel LJ, Jansen DE, Debelak JP, Yull FE, Christman JW, Blackwell TS, Chapman WC 2002 Hepatic cryoablation-induced multisystem injury: bioluminescent detection of NF-κB activation in a transgenic mouse model. J Gastrointest Surg 6:264–270
16. Yull FE, Han W, Jansen ED, Everhart MB, Sadikot RT, Christman JW, Blackwell TS 2003 Bioluminescent detection of endotoxin effects on HIV-1 LTR-driven transcription in vivo. J Histochem Cytochem 51:741–749
17. Safran M, Kim WY, O'Connell F, Flippin L, Gunzler V, Horner JW, Depinho RA, Kaelin Jr WG 2006 Mouse model for noninvasive imaging of HIF prolyl hydroxylase activity: assessment of an oral agent that stimulates erythropoietin production. Proc Natl Acad Sci USA 103: 105–110.
18. Zhang N, Weber A, Li B, Lyons R, Contag PR, Purchio AF, West DB 2003 An inducible nitric oxide synthase-luciferase reporter system for in vivo testing of anti-inflammatory compounds in transgenic mice. J Immunol 170:6307–6319
19. Zhang W, Purchio A, Chen K, Burns SM, Contag CH, Contag PR 2003 In vivo activation of the human CYP3A4 promoter in mouse liver and regulation by pregnane X receptors. Biochem Pharmacol 65:1889–1896
20. Zhang W, Purchio AF, Chen K, Wu J, Lu L, Coffee R, Contag PR, West DB 2003 A transgenic mouse model with a luciferase reporter for studying in vivo transcriptional regulation of the human CYP3A4 gene. Drug Metab Dispos 31:1054–1064
21. O'Connell-Rodwell CE, Shriver D, Simanovskii DM, McClure C, Cao YA, Zhang W, Bachmann MH, Beckham JT, Jansen ED, Palanker D, Schwettman HA, Contag CH 2004 A genetic reporter of thermal stress defines physiologic zones over a defined temperature range. FASEB J 18:264–271
22. Zhang N, Fang Z, Contag PR, Purchio AF, West DB 2004 Tracking angiogenesis induced by skin wounding and contact hypersensitivity using a Vegfr2-luciferase transgenic mouse. Blood 103:617–626
23. Francis GA, Fayard E, Picard F, Auwerx J 2003 Nuclear receptors and the control of metabolism. Annu Rev Physiol 65:261–311
24. Shulman AI, Mangelsdorf DJ 2005 Retinoid X receptor heterodimers in the metabolic syndrome. N Engl J Med 353:604–615
25. Ciana P, Di Luccio G, Belcredito S, Pollio G, Vegeto E, Tatangelo L, Tiveron C, Maggi A 2001 Engineering of a mouse for the *in vivo* profiling of estrogen receptor activity. Mol Endocrinol 15:1104–1113
26. Ciana P, Raviscioni M, Mussi P, Vegeto E, Que I, Parker MG, Lowik C, Maggi A 2003 In vivo imaging of transcriptionally active estrogen receptors. Nat Med 9:82–86
27. Ye X, Han SJ, Tsai SY, DeMayo FJ, Xu J, Tsai MJ, O'Malley BW 2005 Roles of steroid receptor coactivator (SRC)-1 and transcriptional intermediary factor (TIF) 2 in androgen receptor activity in mice. Proc Natl Acad Sci USA 102:9487–9492
28. Makishima M, Okamoto AY, Repa JJ, Tu H, Learned RM, Luk A, Hull MV, Lustig KD, Mangelsdorf DJ, Shan B 1999 Identification of a nuclear receptor for bile acids. Science 284:1362–1365
29. Parks DJ, Blanchard SG, Bledsoe RK, Chandra G, Consler TG, Kliewer SA, Stimmel JB, Willson TM, Zavacki AM, Moore DD, Lehmann JM 1999 Bile acids: natural ligands for an orphan nuclear receptor. Science 284: 1365–1368
30. Wang H, Chen J, Hollister K, Sowers LC, Forman BM 1999 Endogenous bile acids are ligands for the nuclear receptor FXR/BAR. Mol Cell 3:543–553
31. Howard WR, Pospisil JA, Njolito E, Noonan DJ 2000 Catabolites of cholesterol synthesis pathways and forskolin as activators of the farnesoid X-activated nuclear receptor. Toxicol Appl Pharmacol 163:195–202
32. Wang S, Lai K, Moy FJ, Bhat A, Hartman HB, Evans MJ 2006 The nuclear hormone receptor farnesoid X receptor (FXR) is activated by androsterone. Endocrinology 147: 4025–4033
33. Chiang JY 2002 Bile acid regulation of gene expression: roles of nuclear hormone receptors. Endocr Rev 23: 443–463
34. Houten SM, Auwerx J 2004 The enterohepatic nuclear receptors are major regulators of the enterohepatic circulation of bile salts. Ann Med 36:482–491
35. Russell DW 2003 The enzymes, regulation, and genetics of bile acid synthesis. Annu Rev Biochem 72:137–174
36. Thompson JF, Hayes LS, Lloyd DB 1991 Modulation of firefly luciferase stability and impact on studies of gene regulation. Gene 103:171–177
37. Ghoda L, van Daalen Wetters T, Macrae M, Ascherman D, Coffino P 1989 Prevention of rapid intracellular degradation of ODC by a carboxyl-terminal truncation. Science 243:1493–1495
38. Rogers S, Wells R, Rechsteiner M 1986 Amino acid sequences common to rapidly degraded proteins: the PEST hypothesis. Science 234:364–368
39. Li X, Zhao X, Fang Y, Jiang X, Duong T, Fan C, Huang CC, Kain SR 1998 Generation of destabilized green fluorescent protein as a transcription reporter. J Biol Chem 273:34970–34975
40. Leclerc GM, Boockfor FR, Faught WJ, Frawley LS 2000 Development of a destabilized firefly luciferase enzyme for measurement of gene expression. Biotechniques 29: 590–591, 594–596, 598
41. Chung JH, Whiteley M, Felsenfeld G 1993 A 5′ element of the chicken β-globin domain serves as an insulator in human erythroid cells and protects against position effect in *Drosophila*. Cell 74:505–514
42. Chung JH, Bell AC, Felsenfeld G 1997 Characterization of the chicken β-globin insulator. Proc Natl Acad Sci USA 94:575–580
43. Wilson C, Bellen HJ, Gehring WJ 1990 Position effects on eukaryotic gene expression. Annu Rev Cell Biol 6:679–714
44. Bell AC, Felsenfeld G 1999 Stopped at the border: boundaries and insulators. Curr Opin Genet Dev 9:191–198
45. Sun FL, Elgin SC 1999 Putting boundaries on silence. Cell 99:459–462
46. Echelard Y, Vassileva G, McMahon AP 1994 Cis-acting regulatory sequences governing Wnt-1 expression in the developing mouse CNS. Development 120: 2213–2224

47. Rowitch DH, Echelard Y, Danielian PS, Gellner K, Brenner S, McMahon AP 1998 Identification of an evolutionarily conserved 110 base-pair cis-acting regulatory sequence that governs Wnt-1 expression in the murine neural plate. Development 125:2735–2746
48. Forman BM, Goode E, Chen J, Oro AE, Bradley DJ, Perlmann T, Noonan DJ, Burka LT, McMorris T, Lamph WW, Evans RM, Weinberger C 1995 Identification of a nuclear receptor that is activated by farnesol metabolites. Cell 81:687–693
49. Bookout AL, Jeong Y, Downes M, Yu RT, Evans RM, Mangelsdorf DJ 2006 Anatomical profiling of nuclear receptor expression reveals a hierarchical transcriptional network. Cell 126:789–799
50. Otte K, Kranz H, Kober I, Thompson P, Hoefer M, Haubold B, Remmel B, Voss H, Kaiser C, Albers M, Cheruvallath Z, Jackson D, Casari G, Koegl M, Paabo S, Mous J, Kremoser C, Deuschle U 2003 Identification of farnesoid X receptor β as a novel mammalian nuclear receptor sensing lanosterol. Mol Cell Biol 23: 864–872
51. Goodwin B, Jones SA, Price RR, Watson MA, McKee DD, Moore LB, Galardi C, Wilson JG, Lewis MC, Roth ME, Maloney PR, Willson TM, Kliewer SA 2000 A regulatory cascade of the nuclear receptors FXR, SHP-1, and LRH-1 represses bile acid biosynthesis. Mol Cell 6:517–526
52. Lu TT, Makishima M, Repa JJ, Schoonjans K, Kerr TA, Auwerx J, Mangelsdorf DJ 2000 Molecular basis for feedback regulation of bile acid synthesis by nuclear receptors. Mol Cell 6:507–515
53. Inagaki T, Choi M, Moschetta A, Peng L, Cummins CL, McDonald JG, Luo G, Jones SA, Goodwin B, Richardson JA, Gerard RD, Repa JJ, Mangelsdorf DJ, Kliewer SA 2005 Fibroblast growth factor 15 functions as an enterohepatic signal to regulate bile acid homeostasis. Cell Metab 2:217–225
54. Lee H, Zhang Y, Lee FY, Nelson SF, Gonzalez FJ, Edwards PA 2006 FXR regulates organic solute transporters α and β in the adrenal gland, kidney, and intestine. J Lipid Res 47:201–214
55. Nagy A, Gertsenstein M, Vintersten K, Behringer R 2003 Manipulating the mouse embryo. Cold Spring Harbor, NY: Cold Spring Harbor Laboratory Press

Molecular Endocrinology **is published monthly by The Endocrine Society (http://www.endo-society.org), the foremost professional society serving the endocrine community.**